



Article

# Human Activities Inducing High CH<sub>4</sub> Diffusive Fluxes in an Agricultural River Catchment in Subtropical China

Hongbao Wu <sup>1</sup>, Qiang Zhao <sup>2</sup>, Qingzhu Gao <sup>1</sup>, Yu'e Li <sup>1</sup>, Yunfan Wan <sup>1</sup>, Yong Li <sup>3</sup>, Di Tian <sup>4</sup>, Yulin Liao <sup>5</sup>, Meirong Fan <sup>6</sup>, Hasbagan Ganjurjav <sup>1</sup>, Guozheng Hu <sup>1</sup>, Bin Wang <sup>1</sup>, Xuan Chen <sup>1</sup> and Xiaobo Qin <sup>1,\*</sup>

<sup>1</sup> Institute of Environment and Sustainable Development in Agriculture, Chinese Academy of Agricultural Sciences, Beijing 100081, China

<sup>2</sup> School of Geography and Tourism, Anhui Normal University, Wuhu 241000, China

<sup>3</sup> Key Laboratory of Agro-ecological Processes in Subtropical Region, Institute of Subtropical Agriculture, Chinese Academy of Sciences, Changsha 410125, China

<sup>4</sup> College of Life Sciences, Capital Normal University, Beijing 100048, China

<sup>5</sup> Soils and Fertilizer Institute of Hunan Province, Changsha 410125, China

<sup>6</sup> Changsha Environmental Protection College, Changsha 410004, China

\* Correspondence: qinxiaobo@caas.cn

Received: 15 January 2020; Accepted: 2 March 2020; Published: 9 March 2020



**Abstract:** Methane (CH<sub>4</sub>) is one of the key greenhouse gases (GHGs) in the atmosphere with current concentration of 1859 ppb in 2017 due to climate change and anthropogenic activities. Rivers are of increasing concern due to sources of atmospheric CH<sub>4</sub>. However, knowledge and data limitations exist for field studies of subtropical agricultural river catchments, particularly in southern China. The headspace balance method and the diffusion model method were employed to assess spatiotemporal variations of CH<sub>4</sub> diffusive fluxes from April 2015 to January 2016 in four order reaches (S1, S2, S3, and S4) of the Tuoqia River, Hunan, China. Results indicated that both the dissolved concentrations and diffusive fluxes of CH<sub>4</sub> showed obvious spatiotemporal variations. The observed mean concentration and diffusive flux of CH<sub>4</sub> were  $0.40 \pm 0.02 \mu\text{mol L}^{-1}$  and  $41.19 \pm 2.50 \mu\text{g m}^{-2} \text{h}^{-1}$ , respectively, showing the river to be a strong source of atmospheric CH<sub>4</sub>. The CH<sub>4</sub> diffusive fluxes during the rice-growing seasons were significantly greater than the winter fallow season (an increase of 80.26%). The spatial distribution of CH<sub>4</sub> diffusive fluxes increased gradually from  $(17.58 \pm 1.42)$  to  $(55.56 \pm 4.32) \mu\text{g m}^{-2} \text{h}^{-1}$  due to the organic and nutrient loading into the river waterbodies, with the maximum value at location S2 and the minimum value at location S1. Correlation analysis showed that the CH<sub>4</sub> diffusive fluxes exhibited a positive relationship with the dissolved organic carbon (DOC), salinity, and water temperature (WT), while a negative correlation occurred between CH<sub>4</sub> diffusive fluxes and the dissolved oxygen (DO) concentration, as well as the pH value. Our findings highlighted that a good understanding of exogenous nutrient loading in agricultural catchments will clarify the influence of human activities on river water quality and then constrain the global CH<sub>4</sub> budget.

**Keywords:** CH<sub>4</sub> diffusive fluxes; spatiotemporal variation; agricultural catchment; river network; human activities

## 1. Introduction

Methane (CH<sub>4</sub>) is a powerful greenhouse gas (GHG), which has a 28 times greater global warming potential (GWP) than carbon dioxide (CO<sub>2</sub>) over a 100-year time period [1], accounting for

approximately 20% of the radiative forcing added to the atmosphere [2]. Therefore, when GWP is expressed in CO<sub>2</sub> equivalents, CH<sub>4</sub> is an important contributor to GHG emissions [3]. The current global concentration of atmospheric CH<sub>4</sub> (~1859 ppb) reached 257% of the preindustrial level (~722 ppb) due to increased emissions from anthropogenic sources and, at present, is increasing by 7 ppb percent year [4]. In addition, as a consequence of increasing CH<sub>4</sub> concentrations, global atmospheric temperature will rise by 1.5–4.8 °C by the end of this century [1]. Terrestrial freshwater has been well documented as a major source of atmospheric CH<sub>4</sub>. The global CH<sub>4</sub> emission rate from global freshwater is estimated to be 26.8–103.3 Tg yr<sup>-1</sup>, accounting for a significant share of 50% of anthropogenic CH<sub>4</sub> emissions to the atmosphere [5–7]. However, recent studies have shown that CH<sub>4</sub> emissions from freshwater are the most uncertain component of this current estimate of terrestrial freshwater systems, primarily due to the small amount of data, limited geographic distribution of measurements, and the great diversity of hydrology and climates across terrestrial freshwaters [3,8], particularly in the riverine types, which vary in terms of different CH<sub>4</sub> emissions under different river systems [9]. Therefore, more comprehensive data from riverine areas are required to accurately represent, within global CH<sub>4</sub> budgets, the continental CH<sub>4</sub> fluxes associated with terrestrial rivers.

Across the world, rivers are impacted by urbanization and industrialization, and they are generally highly variable in terms of CH<sub>4</sub> emissions [10–12]. Up to now, few measurements of CH<sub>4</sub> fluxes from rivers impacted by agriculture (rice paddies) have been reported, despite being an anthropogenic source of CH<sub>4</sub> [8]. Previous studies have shown that CH<sub>4</sub> emissions from riverine areas are close to levels of organic material and nutrient inputs [7,8,13], whose high nutrient levels (available carbon and nitrogen) and sediment loads can synergistically enhance the activity of microorganisms [14] and, as a consequence, these environments contribute significantly to CH<sub>4</sub> emissions. Rivers draining into agricultural watersheds, particularly in rice cultivation, increase the availability of nutrients in rivers via drainage, leaching, runoff, and soil erosion more easily than with rivers that are unaffected by agriculture [15]. Previous studies have suggested that organic carbon (DOC), ammonium nitrogen (NH<sub>4</sub><sup>+</sup>-N), and nitrate nitrogen (NO<sub>3</sub><sup>-</sup>-N) have increased from the river draining rice paddy watershed with the increase of Strahler stream order [16,17]. Recent research has attempted to quantify irrigation-induced CH<sub>4</sub> emissions in the rivers draining into rice paddy watersheds and those that are not impacted by agriculture [8]; however, they exhibit wide variations. Therefore, further investigation is recommended on CH<sub>4</sub> emissions from rivers impacted by agriculture as a key promoter of climate change.

Given that terrestrial freshwater is an important potential source of atmospheric CH<sub>4</sub> and plays a significant role in global CH<sub>4</sub> budgets, the pathways of CH<sub>4</sub> production have therefore received an increasing amount of attention [18]. CH<sub>4</sub>, produced naturally in the sediment under anaerobic conditions via microbial processes, can be transported to the atmosphere by molecular diffusion, bubble ebullition, and plant-mediated transportation [6]. Numerous studies have reported the pathways responsible for CH<sub>4</sub> production in terrestrial freshwater, which include fermentation of acetate and reduction of carbon dioxide [18,19]. Numerous studies have demonstrated that the pathways of CH<sub>4</sub> production are affected by temperature, acid concentration, pH, and nutrient levels [18–22]. At a low acetate concentration (50 mmol L<sup>-1</sup>), acetoclastic methanogenesis dominated, regardless of the ammonium concentration, while at higher acetate concentrations (150 and 250 mmol L<sup>-1</sup>) and at low–medium ammonium levels (1–4 g N L<sup>-1</sup>), hydrogenotrophic methanogenesis dominated [19]. Surveys such as those conducted by Holmes et al. (2013) [18] showed that in nutrient-poor soil, amounts of CH<sub>4</sub> were produced via acetate fermentation, while at the nutrient-impacted site, the proportion of CH<sub>4</sub> produced via hydrogenotrophic methanogenesis increased from 25% to 50%.

China is now the second largest region for rice cultivation and the largest producer of rice in the world, accounting for approximately 20% the world's rice-producing area and 28.1% of global rice production [23–25]. Simultaneously, a consequence of extensive rice cultivation, China is the country with the largest amount of irrigation in the world [23]. In addition, China also has one of the largest amounts of pig breeding in the world, with approximately 42,800 pigs situated there in 2018 [26].

However, Hunan, a central province of China, is a traditional and major area of rice cultivation and grain production, and it has the second largest annual output of pigs in China [27]. In order to increase the crop grain yields draining into a subtropical rice paddy in China, large amounts of nitrogen fertilizer and frequent irrigation are applied in the rice paddies. However, excessive use of nitrogen has led to decreasing nitrogen use efficiency, and unused N from drainage and runoff flows may be transported to rivers and increase sediment loading and nutrient enrichment, resulting in water pollution and CH<sub>4</sub> emissions [16,17,28,29]. Rice paddies have been identified as a source of atmospheric CH<sub>4</sub>, and as much as 50% of dissolved CH<sub>4</sub> in soils and drainage water can also be transported into rivers that are draining into rice paddy watersheds [29,30]. Moreover, livestock and poultry breeding can annually produce as many as 380 million tons of manure and wastewater and may contribute 1.78–2.68 Tg CH<sub>4</sub> yr<sup>-1</sup> outgassing to the atmosphere in China [31,32]. Moreover, when high carbon and nitrogen inputs change dissolved oxygen, pH, and microbial activity and population structures in soils and water, the pathways of CH<sub>4</sub> production will change dramatically [14,18,33,34]. Unfortunately, rivers impacted by agriculture (rice planting and livestock breeding) as an anthropogenic source of CH<sub>4</sub> are poorly represented in the subtropical region, China, particularly in the pathways of CH<sub>4</sub> production. However, up to now, the above situation is still uncertain.

Therefore, to clarify CH<sub>4</sub> diffusive fluxes in rivers draining into a rice paddy watershed affected by agriculture, a 10-month field measurement was undertaken to examine the effects of anthropogenic activities on CH<sub>4</sub> diffusive fluxes in Changsha, Hunan Province, China. In the present study, CH<sub>4</sub> emissions were measured by the headspace balance method and the diffusion model method. The main objectives of this study were first to capture spatiotemporal variations in dissolved concentrations and diffusive fluxes of CH<sub>4</sub> from rivers draining into rice paddy watersheds. Then, we aimed to examine the dependence of CH<sub>4</sub> diffusive fluxes on water parameters and nutrients. Finally, we also attempted to reveal the main pathway of CH<sub>4</sub> production in terrestrial rivers impacted by agriculture.

## 2. Materials and Methods

### 2.1. Experimental Sites

The Tuoqia River, a tributary of the Xiangjiang River, represents a typical river impacted by agriculture in subtropical central China. The study is located in Changsha, Hunan Province, China (112°56′–113°36′E, 27°55′–28°40′N), with a 52.10 km<sup>2</sup> area and an elevation ranging from 56 m to 434.8 m above sea level from the estuary to headwaters [35]. The experimental area represented a typical subtropical humid monsoon climate, with an annual mean air temperature of 17.2 °C and precipitation of 1300 mm. Most of the rainfall occurs from April to July due to moist summer monsoons, with the precipitation in this period accounting for approximately 70% of the total annual rainfall. The study area is a typical hilly, agricultural catchment in subtropical central China, where forest and paddy fields are the main land use types, accounting for 33% and 61.1% of the total catchment area, respectively [36,37]. The experimental area has been dominated by paddy rice-cropping systems for hundreds of years, with high amounts of organic materials and nitrogen fertilizer inputs (typically applied at a fertilization rate of ~374 kg hm<sup>-2</sup> yr<sup>-1</sup>) [27]. In general, early rice is planted in mid-April and harvested in mid-July, while late rice is planted in late July and harvested in late October in the experimental area. Midseason drainage and moist irrigation episodes are currently practiced in rice paddies. In addition, the whole catchment area has a population of approximately 28,000, and the 60 farmers and urban residents surveyed have approximately 500 poultry and 500 pigs [35]. Of specific interest is the density of average breeding being as high as 3.46 AU hm<sup>-2</sup> [27]. Moreover, there are dense settlements and scattered small factories and livestock farms along the river valley. The sampling area is about 10 km from upstream to downstream of the river, the water body is 5 m wide, and the water depth ranges from 0.1 m to 1 m.

## 2.2. Sample Design and Collection

Surface water samples were collected weekly at 20 cm below the surface from the Tuoja River over a 10-month period (April 2015 to January 2016) and analyzed for dissolved CH<sub>4</sub> concentrations and other water parameters. According to the grading characteristics of the river system and land use types of the catchment, four order reaches were identified along the Tuoja River (S1, S2, S3, and S4) from the origin to the estuary, and twelve locations (Figure 1) were selected for sampling along the four reaches, with every three locations representing the upstream, midstream, and downstream section in each reach, respectively. The four reaches were S1, S2, S3, and S4, in which S1 included numbers 1, 2, and 3, S2 included numbers 4, 5, and 6, S3 included numbers 7, 8, and 9, and S4 included numbers 10, 11, and 12 [36].

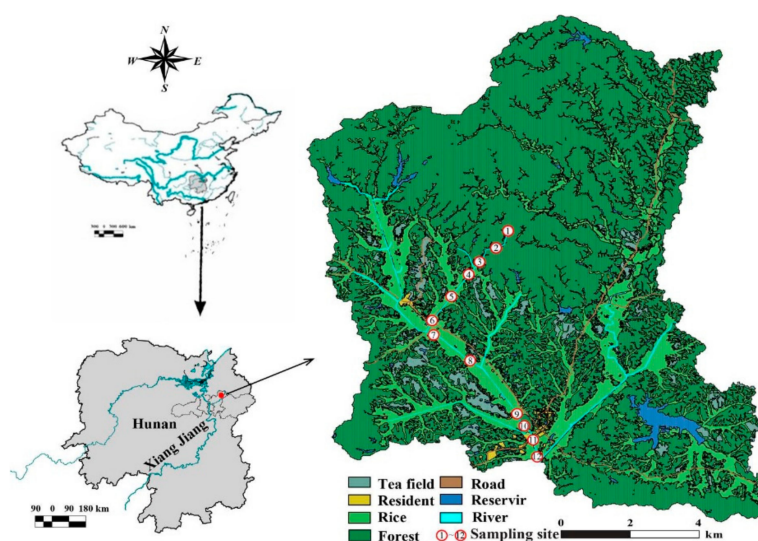


Figure 1. Geographical location and sampling points of research site [36].

To prevent the temperature being able to affect CH<sub>4</sub> emission rates and other parameters, water samples were taken from the Tuoja River using a bucket within the 09:00–11:00 period (UTC + 8). Three replicate water samples were transferred from the bucket to sample bottles and medical syringes to avoid bubbling from the dissolved methane and nutrient elements analyses, respectively. Samples for determining ammonium (NH<sub>4</sub><sup>+</sup>–N), nitrate (NO<sub>3</sub><sup>–</sup>–N), and dissolved organic carbon (DOC) concentrations were collected using 300 mL serum bottles, while samples for dissolved CH<sub>4</sub> analysis were collected in 60 mL medical syringes. Then, 0.5 mL of saturated HgCl<sub>2</sub> solution (10 mg L<sup>–1</sup>) was added to the water samples to stop biological activity [38]. At the same times and locations, several auxiliary measures were taken in parallel with the water samples including river temperature, dissolved oxygen (DO), pH value, and salinity by a calibrated portable handheld meter (Thermo Scientific, Singapore). The wind speeds were obtained by a wind monitor at about 10 m above the river surface. Immediately after sample collection, all syringes and bottles were sent to a laboratory for analysis within 3 hours. If they were not analyzed on the same day, the samples were stored in the dark at 4 °C until required for analysis.

In July and August of 2016, we investigated 60 local farmers and community and village committees and obtained information from the Tuoja River Catchment on population, livestock, poultry, agricultural production, and other relevant information.

## 2.3. Dissolved CH<sub>4</sub> Concentration

The headspace equilibrium method was used to measure the dissolved CH<sub>4</sub> concentrations. The 30-mL water samples in the syringes were accurately replaced by 30 mL of ultrahigh-purity helium gas (>99.999%) in the lab and were subsequently shaken for 10 minutes (on an oscillator)

before standing for 5 minutes so the samples could reach equilibrium. Gases in the headspace were then manually and gently injected into a pre-evacuated vial (12 mL, Labco, UK) and automatically analyzed within 72 hours of collection by using a gas chromatographer (Agilent 7890A, USA) equipped with a Flame Ionization Detector (using 99.999% N<sub>2</sub> as the carrier gas) and a microelectron capture detector (using 99.999% N<sub>2</sub> and 10% CO<sub>2</sub> + 90% N<sub>2</sub> as the carrier gas and backup gas, respectively). The accuracy of the CH<sub>4</sub> and N<sub>2</sub>O measurements were within ±3% and had detection limits of ~0.001 µg L<sup>-1</sup> and ~0.0008 µg L<sup>-1</sup>, respectively.

#### 2.4. CH<sub>4</sub> Diffusive Fluxes

Exchange fluxes of CH<sub>4</sub> from river water bodies to the atmosphere were estimated by the double-layer diffusive model method, as previously reported by Liss & Merlivat (1986) [39] (their Equation (1)) [40] (Zhang et al., 2016). The original CH<sub>4</sub> concentration before equilibrium was calculated using the headspace balancing method, where the diffusive flux was calculated based on an estimation of the gas exchange rate ( $K_w$ ) by using the wind speed ( $U_{10}$ ) with the Schmidt coefficient ( $Sc$ ) [41] (Table 1). The detailed calculation processes for dissolved CH<sub>4</sub> concentration and its exchange flux is provided in previous studies and presented briefly here:

$$F = c \cdot K_w (C_{obs} - C_{eq}) \quad (1)$$

where  $F$  is the diffusive flux of CH<sub>4</sub> between the water surface and the atmosphere (µmol m<sup>-2</sup> h<sup>-1</sup>),  $c$  is a dimensional coefficient,  $K_w$  is the gas exchange rate of CH<sub>4</sub> from the water surface to the atmosphere (cm S<sup>-1</sup>),  $C_{obs}$  is the dissolved CH<sub>4</sub> concentration in the surface water before equilibrium (µmol L<sup>-1</sup>), and  $C_{eq}$  is the dissolved CH<sub>4</sub> concentration at the balance situation, in which the partial air pressure is equal to the water pressure under the actual water temperature (µmol L<sup>-1</sup>).

**Table 1.** The model  $K_w$  values of the CH<sub>4</sub> fluxes in the Tuoja River.

$K_W$ Models	Formula	Wind $U_{10}$ (m s <sup>-1</sup> )	References
LM86	$K_W = 0.17 \times U_{10}(Sc/600)^{-2/3}$	$0 < U_{10} \leq 3.6$	[39]
	$K_W = (2.85 \times U_{10} - 9.65)(Sc/600)^{-1/2}$	$3.6 < U_{10} \leq 13$	
W92a	$K_W = (5.9 \times U_{10} - 49.3)(Sc/600)^{-1/2}$	$U_{10} > 13$	[42]
W92b	$K_W = 0.39 \times U_{10}^2 (Sc/660)^{-1/2}$	Long term $U_{10}$	
RC01	$K_W = 0.31 \times U_{10}^2 (Sc/660)^{-1/2}$	Short term $U_{10}$	[41]
	$K_W = 1.91 \exp(0.35U_{10})(Sc/600)^{-1/2}$	Arbitrarily $U_{10}$	

#### 2.5. Environmental Parameters

The determination of the water quality parameters was carried out simultaneously with the collection of the water samples. The dissolved oxygen (DO), water temperature (WT, in units of °C), pH, electric conductivity (EC), and total dissolved solids (TDSs) were measured in situ with a portable multi-parameter water quality instrument (Thermo Scientific, Singapore). The concentrations of nitrate nitrogen (NO<sub>3</sub><sup>-</sup>-N) and ammonium nitrogen (NH<sub>4</sub><sup>+</sup>-N) were determined by using a flow injection AA3 HR AutoAnalyser (Seal, Germany), which has a coefficient of variation of 0.2% and a detection limit of 0.003 mg N L<sup>-1</sup>. The dissolved organic carbon (DOC) content was analyzed with a total organic carbon analyzer (TOC-Vwp, Shimadzu, Japan), which has a detection range of 0–3000 mg L<sup>-1</sup> and a limit of 2 µg L<sup>-1</sup>. The meteorological data were obtained from a weather station installed in the catchment area (InteliMent Advantage, Dynamax, Inc., USA).

#### 2.6. Statistical Analysis

Statistical analyses were performed using the IBM SPSS 17.0 software package, Excel 2013, and R 2.1.1.1. Linear and nonlinear regressions were applied to test the relationship between the CH<sub>4</sub>



fluxes and the environmental factors. A one-way analysis of variance was used to examine the effects of the river's water quality on the CH<sub>4</sub> fluxes. This was followed by calculating the least significant difference at the 0.05 significance level.

### 3. Results

#### 3.1. Precipitation, Air Temperature, and Wind Speed

Over the 10 months of the study, the precipitation, air temperature, and wind speed showed clear seasonal patterns. The total precipitation was 1185.59 mm during the experimental period, and the precipitation was mainly concentrated from April to July (Figure 2a). The mean air temperature and wind speed were 18.78 °C and 1.15 m s<sup>-1</sup>, respectively (Figure 2a–b). There was no significant difference in monthly average wind speed (Figure 2b).

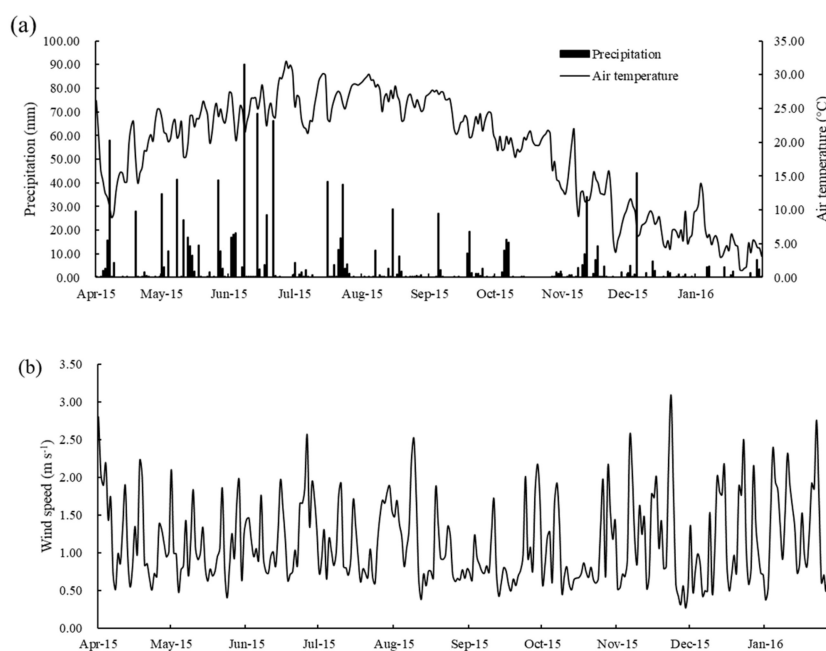


**Figure 2.** Precipitation, air temperature, and wind speed from April 2015 to January 2016. Subfigure explanation: (a) represents precipitation and air temperature; (b) represents wind speed.

#### 3.2. Water Parameters

Spatially, the average value variations of water parameters are shown in Table 2. Except for pH and water temperature, all other water parameters showed a certain spatial variation difference between the spatial samplings. During the sampling reaches, surface water pH was found to be close to neutral (mean value of  $6.83 \pm 0.01$ ), with a variation from  $6.77 \pm 0.07$  to  $6.88 \pm 0.08$ . Spatial concentrations of dissolved organic carbon (DOC) and nitrate nitrogen (NO<sub>3</sub><sup>-</sup>-N) showed similar variation patterns, while dissolved oxygen (DO) was contrary to that of DOC and NO<sub>3</sub><sup>-</sup>-N. Across the sampling reaches, concentrations of DOC and NO<sub>3</sub><sup>-</sup>-N averaged  $2.74 \pm 0.09$  mg L<sup>-1</sup> and  $1.55 \pm 0.03$  mg L<sup>-1</sup>, ranging from  $1.11 \pm 0.09$  to  $3.74 \pm 0.19$  mg L<sup>-1</sup> and from  $0.84 \pm 0.04$  to  $1.85 \pm 0.05$  mg L<sup>-1</sup> in S1 to S4, respectively. Over a 10-month period, the mean DO content of 140 measurements was  $7.45 \pm 0.09$  mg L<sup>-1</sup> over the four sampling reaches, with the highest at location reach S1 and lowest at location reach S2, and with an average of  $8.21 \pm 0.12$  mg L<sup>-1</sup> and  $7.03 \pm 0.21$  mg L<sup>-1</sup>, respectively. The water temperature fluctuated slightly within the experimental period and the sites, ranging from  $18.90 \pm 0.51$  to  $20.06 \pm 0.67$  °C, showing the highest in S3 and the lowest in S1. The lowest NH<sub>4</sub><sup>+</sup>-N concentration occurred in S1 and the highest occurred in S2, with averages of  $0.28 \pm 0.05$  mg L<sup>-1</sup> and  $0.90 \pm 0.09$  mg L<sup>-1</sup>, respectively.

**Table 2.** Water quality parameters in the Tuojia River basin.

Reach	pH	DO (mg L <sup>-1</sup> )	Salinity	WT (°C)	DOC (mg L <sup>-1</sup> )	NH <sub>4</sub> <sup>+</sup> -N (mg L <sup>-1</sup> )	NO <sub>3</sub> <sup>-</sup> -N (mg L <sup>-1</sup> )
S1	6.88 ± 0.08	8.21 ± 0.12	0.03 ± 0.001	18.90 ± 0.51	1.11 ± 0.09	0.28 ± 0.05	0.84 ± 0.04
S2	6.82 ± 0.07	7.03 ± 0.21	0.06 ± 0.001	19.73 ± 0.62	2.81 ± 0.13	0.90 ± 0.09	1.72 ± 0.08
S3	6.77 ± 0.07	7.18 ± 0.19	0.06 ± 0.001	20.06 ± 0.67	3.30 ± 0.16	0.66 ± 0.05	1.78 ± 0.05
S4	6.85 ± 0.07	7.35 ± 0.17	0.07 ± 0.001	19.60 ± 0.65	3.74 ± 0.19	0.67 ± 0.06	1.85 ± 0.05
Mean	6.83 ± 0.01	7.45 ± 0.09	0.06 ± 0.001	19.57 ± 0.31	2.74 ± 0.09	0.63 ± 0.03	1.55 ± 0.03

### 3.3. Water Quality Parameters and Socioeconomic Data

Socioeconomic survey data in 2016 from the Tuojia River Catchment are shown in Table 3. In the catchment there was a total population of 28,234, with populations of 36, 3863, 2739, and 21,776 in S1, S2, S3, and S4, respectively. Pig and poultry quantities were highest at location S2, with values of 426 and 365, respectively. As for the paddy rice-cropping area, the average applied rate of nitrogen fertilizer was 142.5 kg ha<sup>-1</sup> during the rice-growing season. Unfortunately, we did not succeed in obtaining information on pigs, poultry, synthetic and nitrogen fertilizers in S1, and pigs and poultry in S2.

**Table 3.** Socioeconomic survey data in the Tuojia River (the results of pig, poultry, and nitrogen fertilizer were from 60 farmers and urban residents; the result of population was from the whole catchment).

Reach	Population	Pig	Poultry	Nitrogen fertilizer (kg ha <sup>-1</sup> )
S1	36	N/A	16	N/A
S2	3863	426	365	150
S3	2739	82	131	135
S4	21,776	N/A	N/A	142.5

### 3.4. CH<sub>4</sub> Concentration and Flux

Spatiotemporal variations of dissolved CH<sub>4</sub> concentrations and diffusive fluxes are shown in Figures 3 and 4, respectively. The dissolved CH<sub>4</sub> concentrations varied widely at the four order reaches monitored during the experimental period, with the maximum value of dissolved CH<sub>4</sub> concentration with 3.01 µmol L<sup>-1</sup> at location S2 on July 11, 2015 and the minimum with 0.004 µmol L<sup>-1</sup> at location S2 and S1 on January 16, 2016. Simultaneously, we found that significant differences between dissolved CH<sub>4</sub> concentrations were affected by the sampling time, with the highest in the late rice growing period (August to October 2015), followed by the early rice growing period (April to July 2015) and the fallow period (November 2015 to January 2016). Spatially, the sampling position also had a significant effect on the dissolved CH<sub>4</sub> concentrations. In general, the spatial distribution of dissolved CH<sub>4</sub> concentrations increased volatility with the sampling position from the estuary to the river's source. As a comparison, from upstream to downstream, the average observed dissolved CH<sub>4</sub> concentrations were 0.17 ± 0.01, 0.54 ± 0.04, 0.45 ± 0.03 µmol L<sup>-1</sup>, and 0.42 ± 0.03 µmol L<sup>-1</sup> for S1, S2, S3, and S4, respectively. It can clearly be seen that the dissolved CH<sub>4</sub> concentrations in S1 were significantly lower than the other reaches from all the experimental data above (Figure 3, *p* < 0.05).

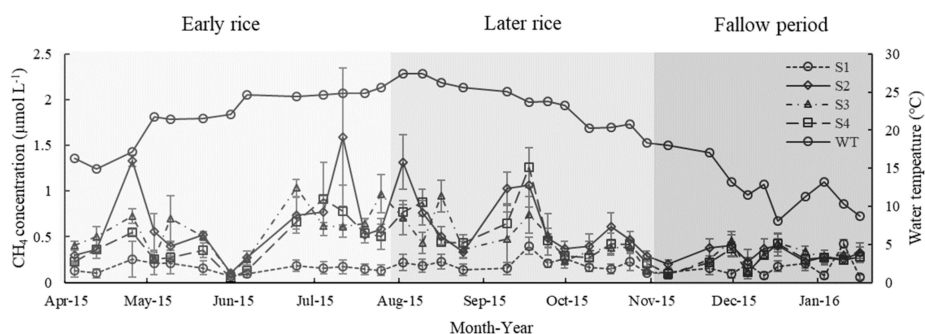


**Figure 3.** Spatiotemporal variations of dissolved CH<sub>4</sub> concentrations in the Tuojia River.

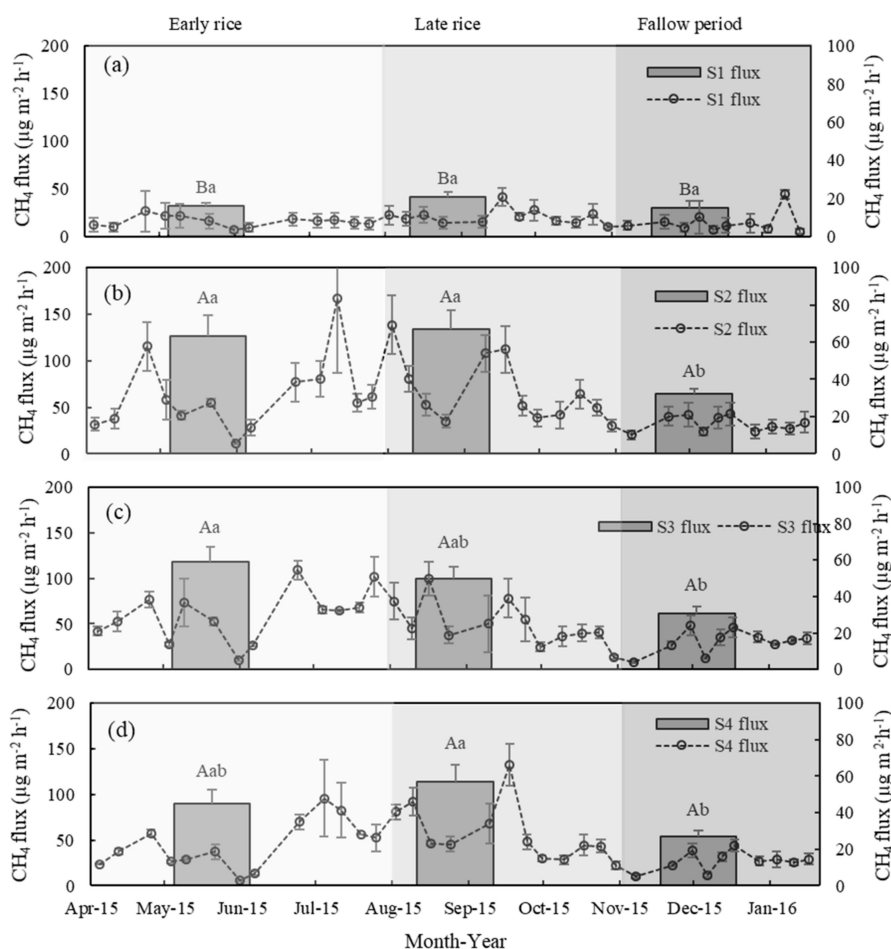


**Figure 4.** Spatiotemporal variations of CH<sub>4</sub> diffusive fluxes in the Tuojia River (lower case above column represents significant differences for the same river reach in different sampling periods; upper case letters above column represent significant differences for the same sampling period in different river reaches). Subfigure explanation: (a) represents S1 CH<sub>4</sub> diffusive fluxes; (b) represents S2; (c) represents S3; (d) represents S4.

According to the dissolved CH<sub>4</sub> concentrations from S1 to S4, the river to the atmospheric CH<sub>4</sub> diffusive fluxes were estimated with the double-layer diffusion model method. The sampling period and position also had significant effects on CH<sub>4</sub> diffusive fluxes. Similarly, in the present study, we also found that CH<sub>4</sub> diffusive fluxes had the same variation patterns as dissolved concentration variation. Among the sampling sites at the four reaches, the diffusive flux of CH<sub>4</sub> was also at its highest value in reach S2 on July 11, 2015, and the lowest value occurred in reach S1 on January 16, 2016, with an average of  $167.26 \pm 79.89$  and  $5.91 \pm 2.99$   $\mu\text{g m}^{-2} \text{h}^{-1}$ , respectively (Figure 4b). The average CH<sub>4</sub> diffusive



fluxes were  $55.56 \pm 4.32$ ,  $47.70 \pm 3.01$ , and  $43.92 \pm 3.14 \mu\text{g m}^{-2} \text{h}^{-1}$ , in reach S2, S3, and S4, which was significantly higher by 215.99%, 171.26%, and 149.77% than S1, respectively. In addition, except for reach S1, the  $\text{CH}_4$  diffusive fluxes were significantly higher during the early and late rice-growing seasons of S2, S3, and S4 compared with those during the fallow period. Nevertheless, there was no significant difference between the early rice and late rice seasons (Figures 4 and 5,  $p < 0.05$ ).

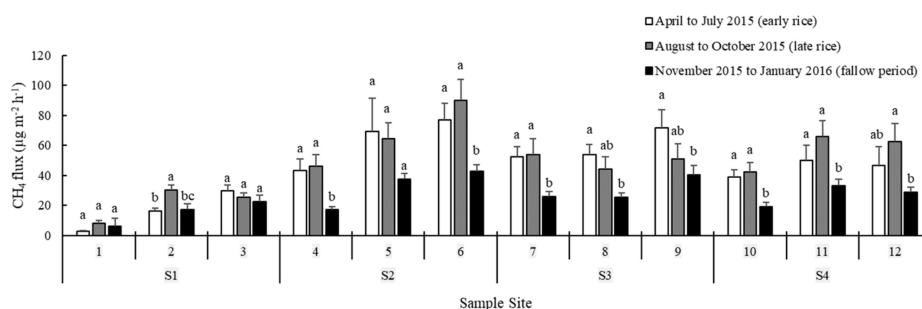


**Figure 5.** Spatiotemporal variations of  $\text{CH}_4$  diffusive fluxes in the Tuojia River.

### 3.5. Dependence of $\text{CH}_4$ Fluxes on Water Parameters

Numerous studies have demonstrated that the  $\text{CH}_4$  fluxes were inevitably affected by water quality (e.g., DOC,  $\text{NH}_4^+\text{-N}$ ,  $\text{NO}_3^-\text{-N}$ , DO, pH value, and water temperature), which affects the production, oxidation, and transport of  $\text{CH}_4$ . By pooling measurements over the 10 months, the  $\text{CH}_4$  diffusive fluxes were positively related to DOC ( $r = 0.47$ ,  $p < 0.001$ ), salinity ( $r = 0.46$ ,  $p < 0.001$ ), and temperature ( $r = 0.27$ ,  $p < 0.01$ ), while they were negatively related to DO concentrations ( $r = -0.49$ ,  $p < 0.001$ ) and pH value ( $r = -0.20$ ,  $p < 0.05$ ) (Figure 6).

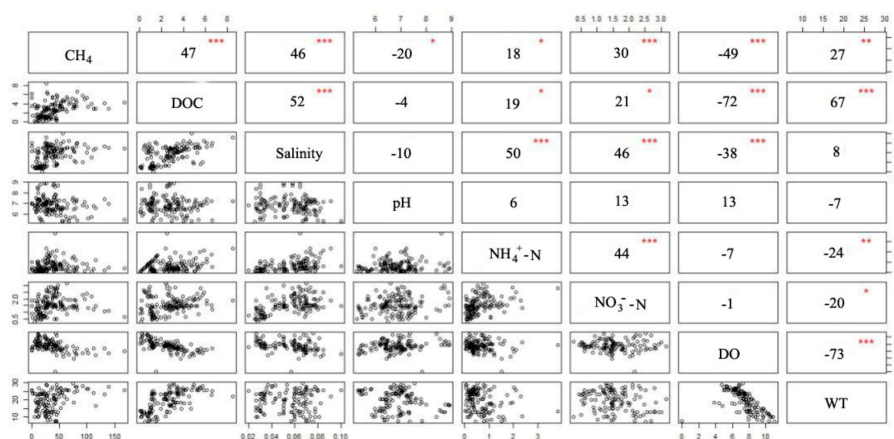


**Figure 6.** Correlation matrices among  $\text{CH}_4$  diffusive fluxes and water parameters (lower-left panel represents scatter diagram, upper-right panel represents  $r$  (correlation coefficient) \*100; the numbers represent the correlation coefficient between  $\text{CH}_4$  diffusive fluxes and environmental factors; the red asterisks represent significant level ( $p$  values). \*\*\*, \*\*, and \* represents  $p < 0.001$ ,  $p < 0.01$ , and  $p < 0.05$ , respectively).

### 3.6. $\text{CH}_4$ Production Pathway

Acetate fermentation and carbon dioxide reduction have been identified as the main processes responsible for the production of  $\text{CH}_4$  in rivers. In our case river, we found that acetate fermentation accounted for over 80% of  $\text{CH}_4$  production, while carbon dioxide reduction only accounted for 20% (Table 4) [38].

**Table 4.** CH<sub>4</sub> production pathways [38].

	S1	S2	S3	S4
fermentation of acetate	87%	78%	76%	81%
reduction of carbon dioxide	13%	22%	24%	19%

## 4. Discussion

### 4.1. Comparison with Other Studies

The dissolved concentrations and fluxes of CH<sub>4</sub> from rivers draining into rice paddy watersheds, such as those studied here, have received less attention than concentrations and fluxes of CH<sub>4</sub> in other freshwater ecosystems, particularly rivers impacted by urbanization and industrialization. Encouragingly, recent studies have begun to fill in this knowledge gap in a number of rivers impacted by agriculture [8,34], providing an opportunity for us to place our results in a larger context. In the present study, the positive values of CH<sub>4</sub> diffusive fluxes implied that the Tuoja River draining into rice paddy watersheds could be an atmospheric source of CH<sub>4</sub>, which agreed with the findings of a large number of studies reported previously [34,43–45]. A considerable amount of research has been reported on CH<sub>4</sub> emissions from river networks, and concentrations and fluxes ranged from 0.002 to 150 μmol L<sup>-1</sup> and 17.70 to 4016.67 μg m<sup>-2</sup> h<sup>-1</sup> [10,13,40,45,46], respectively, and our findings were generally within the ranges that have previously been reported in rivers. Compared with previous studies by Koné et al. (2010) [44], Teodoru et al. (2014) [45], and Borges et al. (2018) [34], CH<sub>4</sub> concentrations in this study were significantly greater than the above results, which may mainly be due to the high nutrient loading (DOC and NH<sub>4</sub><sup>+</sup>-N), sedimentation, and algae blooms impacted by agricultural fertilizer applications being able to stimulate methanogenesis in rivers draining into rice paddy catchments [8,16,47]. In addition, exogenous CH<sub>4</sub> inputs were another reason for the higher CH<sub>4</sub> concentrations in this catchment than what had previously been reported in rivers not impacted by agriculture. High dissolved CH<sub>4</sub> in wastewaters that were directly transported to the rivers by surface runoff, drainage flows, and sewage pipelines may contribute to high CH<sub>4</sub> concentrations [8,38,48]. However, compared with the Lixiahe River, a river draining into a subtropical rice paddy catchment, the CH<sub>4</sub> diffusive fluxes (mean of 41.19 μg m<sup>-2</sup> h<sup>-1</sup>) were significantly lower by one to two orders of magnitude than what had previously been reported (3.50 mg m<sup>-2</sup> h<sup>-1</sup>) [8]. One possible important reason for this was the great diversity in topography, discharge, river flow velocity, and irrigation frequency between the Tuoja River agriculture catchment and the Lixiahe River agriculture catchment [8,34,49].

### 4.2. Spatiotemporal Variation in CH<sub>4</sub> Fluxes

The spatial position of the sampling sites had significant effects on CH<sub>4</sub> diffusive fluxes (Figure 4). Similar to the results from Stanley et al. (2016) [7] and Zhang et al. (2016) [40] reported previously, our findings also showed that CH<sub>4</sub> diffusive fluxes were at their lowest values in reach S1, their highest values in reach S2, and the values decreased in a downstream direction in reaches S3 and S4. The spatial pattern of CH<sub>4</sub> diffusive fluxes was generally in agreement with those of DOC, NH<sub>4</sub><sup>+</sup>-N, and NO<sub>3</sub><sup>-</sup>-N, but in contrast with DO (Table 2, Figure 4, and Figure 5). The highest CH<sub>4</sub> diffusive fluxes at location S2 could be primarily ascribed to the nutrient and sediment loads through drainage water, soil erosion, and runoff directly flowing into the S2 reach. Over the 10-month period, the average NH<sub>4</sub><sup>+</sup>-N concentration in S2 was 221.43%, 85.71%, and 82.14% higher than those of S1, S3, and S4, respectively. Theoretically, methanogenic archaea usually depend on NH<sub>4</sub><sup>+</sup> as a direct nitrogen source [50], and NH<sub>4</sub><sup>+</sup>, whose chemical structure resembles that of the CH<sub>4</sub> molecule, can interfere with the oxidation of CH<sub>4</sub> because NH<sub>4</sub><sup>+</sup> competes with CH<sub>4</sub> for CH<sub>4</sub> mono-oxygenase, the key enzyme of CH<sub>4</sub> oxidation [51]. CH<sub>4</sub> production is strongly controlled by DOC content in river, which suggests that the amount of the CH<sub>4</sub> was produced by organic carbon in anoxic river reaches [40]. The water

DOC concentrations generally enhanced with an increase in Strahler stream order, where DOC in S2 was higher than that of S1 by 153.15%. Data from surface water show a significant and positive linear relationship between CH<sub>4</sub> diffusive fluxes and DOC content, with an effect ( $r = 0.47$ ,  $p < 0.001$ ) similar to what Stanley et al. (2017) [7] and Borges et al. (2018) [34] had reported previously. Exogenous DOC inputs caused by rice cultivation and livestock and poultry breeding (Table 3) can decrease the effect of several river microbial processes on their electron donors, resulting in enriched methanogens activity and stimulating more CH<sub>4</sub> production [52]. In addition, increased DOC can enable river aerobic microorganisms to consume more oxygen (O<sub>2</sub>), with the result of the oxidation process being limited to producing a positive effect on CH<sub>4</sub> emissions. Theoretically, the production and consumption of CH<sub>4</sub> occur simultaneously under the action of methanogenic archaea and methane-oxidizing bacteria, and the balance of the two processes determines the CH<sub>4</sub> flux [53–55]. However, water DO plays an important role in the balance of the two processes. Surveys such as those conducted by Kuivila et al. (1989) [56] showed that the carbon cycle in oxic rivers assumes CH<sub>4</sub> production in the sediments and oxidation when CH<sub>4</sub> diffuses from the sediments into the water column. Most CH<sub>4</sub>, however, was oxidized by communities of epiphytic methanotrophs when passing through the oxic water-air interface [57]. Studies previously reported that most of emitted CH<sub>4</sub> can be oxidized from a surface water column to the atmosphere [58,59] (Moreover, Reeburgh et al. (2007) [60] suggested that the value may reach a value as high as 90%. In our case river, we concluded that surface water CH<sub>4</sub> diffusive fluxes in S2 were higher than in the other reaches and were well predicted by DO ( $r = -0.49$ ,  $p < 0.001$ ). Lower DO not only reduced CH<sub>4</sub> oxidation from the water column into the atmosphere but also lowered the redox potential in the sediments, resulting in an increase in CH<sub>4</sub> production potential and the conversion efficiency of a substrate into CH<sub>4</sub>, which in turn facilitated CH<sub>4</sub> emissions [37,40,61]. In addition, our river contained higher amounts of dissolved CH<sub>4</sub> in the wastewater from livestock and poultry farming. Particularly, pig manure wastewater was transported into the reach in S2, resulting in CH<sub>4</sub> fluxes in this reach being higher than in other reaches [31,49]. Therefore, we concluded that higher concentrations of DOC and NH<sub>4</sub><sup>+</sup>-N, lower DO, and exogenous inputs were the main causes of the CH<sub>4</sub> diffusive fluxes in reach S2.

CH<sub>4</sub> diffusive fluxes were also strongly affected by the sampling period (Figure 4). The seasonal dynamics of CH<sub>4</sub> diffusive fluxes from the rivers were typically characterized by a pattern in which CH<sub>4</sub> diffusive fluxes were the lowest in the winter and the highest in the summer (Figure 5). One possible explanation for this was the remarkable difference between ambient variants and nutrients in the rice-growing season and the fallow period [17,30]. Based on a two-year monitoring study of the Lixiahe River affected by agriculture in Jiangsu Province, China, Wu et al. (2019) [8] also showed that CH<sub>4</sub> diffusive fluxes during the rice-growing season (June to October) were higher than those in the winter (December to January), and they further pointed out that the differences were attributed to the higher organic and nutrient loading in the rice-growing season.

During the rice-growing seasons, synthetic fertilizers and nitrogen fertilizer are applied at a rate of 580.35 kg ha<sup>-1</sup> and 142.5 kg ha<sup>-1</sup>, respectively (Table 3). However, the utilization efficiency of nitrogen fertilizer in farmland soil is only 30%–40% [62]. Therefore, this low efficiency and high input plantation mode caused the amount of the unutilized nitrogen to be transported into the river channel through drainages, irrigation, and surface runoff, resulting in enriched organic and nutrient loading and depleted water O<sub>2</sub> in the water and sediment [8,10,16,34]. High nutrient levels were corrected with elevated microbial activity and CH<sub>4</sub> production [63,64]. Surveys such as those conducted by Li et al. (2018) [30] showed that CH<sub>4</sub> fluxes were higher in the rice-growing seasons than in the fallow period; however, Wu et al., (2019) [8] also stated that drainage could greatly reduce CH<sub>4</sub> emissions from rice paddies in this period, with values as high as 50% [29]. Noticeably, this reduction could be offset by increased CH<sub>4</sub> emissions as a consequence of nutrient enrichment and sediment loading in rivers draining into rice paddy watersheds [8]. Therefore, the exogenous inputting of CH<sub>4</sub> was also one of the reasons for the higher CH<sub>4</sub> diffusive fluxes in the river during the rice-growing seasons.

The dissolved CH<sub>4</sub> concentrations increased with water temperature (Figure 4), suggesting that methanogenic archaea were sensitive to temperature [65]. Previous studies indicated that as temperature increased by 10 °C, the methanogen reproduction rate doubled and the CH<sub>4</sub> emission rate increased by  $2.4 \pm 1.0 \text{ mmol m}^{-2} \text{ d}^{-1}$  [65]. Specifically, when the temperature decreased from 30 °C to 15 °C, the CH<sub>4</sub> production rate was sharply reduced [66]. Moreover, a higher temperature also increased the  $K_W$  value, resulting in a faster transfer of CH<sub>4</sub> from the surface water column to the atmosphere [67]. Therefore, as a consequence of higher CH<sub>4</sub> diffusive fluxes in rice-growing seasons, mainly due to the intense nutrient and sediments loads, high water temperatures and low O<sub>2</sub> availability in the river stimulate more CH<sub>4</sub> production [8]. In addition, precipitation not only increased greenhouse gas concentrations by flushing inorganic and organic carbon from the landscape into stream [38,68] but also caused an “initial scouring” effect by precipitation facilitating a high diffusive rate of CH<sub>4</sub> in rivers [69]. In Figures 2–4, we found that the variation of CH<sub>4</sub> diffusive fluxes was generally in agreement with precipitation.

### 4.3. CH<sub>4</sub> Production Pathways

The fermentation of acetate (acetoclastic methanogenesis) and reduction of carbon dioxide (CO<sub>2</sub>, hydrogenotrophic methanogenesis) have been identified as the two main pathways for CH<sub>4</sub> production in terrestrial freshwater [18,19]. Previous studies have reported that approximately 70% of the CH<sub>4</sub> produced can be attributed to acetate fermentation, while carbon dioxide reduction accounted for only 30% [19,70,71]. The findings of the present study were in line with those of Conrad (1999) [70] and Whiticar (1999) [71], which produced CH<sub>4</sub> observed mean values of 80.5% by acetate fermentation and 19.5% by carbon dioxide reduction. The pathways of CH<sub>4</sub> production were affected by ambient variants and nutrient loads (e.g., temperature, pH, acid concentration, and ammonium [18–22]); therefore, the sampling sites had significant effects on the rate of acetate fermentation and carbon dioxide reduction for CH<sub>4</sub> production. In our case river, we found that the proportion of acetoclastic pathways in S1 were higher by 9%, 11%, and 6% than S2, S3, and S4, respectively. In contrast, CO<sub>2</sub> reduction was lower than other reaches (Table 3). One possible explanation was that most of the CH<sub>4</sub> was produced through acetate fermentation [18,19] (not impacted by agriculture in S1 with poor nutrients); at the nutrient-impacted sites (S2, S3, and S4), the larger proportion of CH<sub>4</sub> was produced via hydrogenotrophic methanogenesis (Holmes et al., 2013).

## 5. Conclusions

In summary, this study systematically presented CH<sub>4</sub> diffusive fluxes of the Tuoja River impacted by human activities in subtropical agriculture catchments. Our findings supported the general conclusion that the river was a consistent source of atmospheric CH<sub>4</sub>. Over the 10-month experimental period, we found distinct spatiotemporal variations of CH<sub>4</sub> diffusive fluxes along the Tuoja River catchment, which was generally consistent with the nutrient loading pattern of the river water across the drainage basin. A large amount of rice cultivation and livestock breeding could largely explain the observed CH<sub>4</sub> diffusive flux patterns of the river flows. As a consequence of the described agricultural practice, concentrations of DOC and NH<sub>4</sub><sup>+</sup>-N increased, DO content in river water decreased, and more CH<sub>4</sub> production was stimulated. Therefore, the most valuable conclusion was that the CH<sub>4</sub> diffusive fluxes were mainly concentrated in the rice growing season and the nutrient-impacted river reach. Our findings highlighted that an improved understanding of river water exogenous input draining into agricultural catchments will help clarify the influence of human activities on river water quality and help to better constrain the magnitude of CH<sub>4</sub> and other GHG diffusive fluxes in agricultural catchments.

**Author Contributions:** This paper was written by H.W. in collaboration with all co-authors. The experiments were conducted by H.W. and Q.Z. The writing—original draft preparation was written by H.W. The writing—review and editing was written by H.W. and X.Q. The data was analyzed by H.W., D.T., H.G., B.W. and X.C. The conceptualization and methodology for the research experiment were provided by Q.G., Y.L., Y.W., Y.L., G.H.,

Y.L. and M.F. The project administration and funding acquisition were supervised by X.Q. All authors have read and agreed to the published version of the manuscript.

**Funding:** The financial support from National Natural Science Foundation of China (41775157, 41475129) and National Key Basic Research Program of China (2012CB417106) are gratefully acknowledged.

**Acknowledgments:** The authors thank the journal editor and reviewers for their hard work and constructive suggestions.

**Conflicts of Interest:** The authors declare no conflict of interest.

## References

1. IPCC. *Climate Change 2013: The Physical Science Basis. (Contribution of Working Group I to the Fifth Assessment Report of the Intergovernmental Panel on Climate Change)*; Cambridge University Press: Cambridge, UK, 2013.
2. Kirschke, S.; Bousquet, P.; Ciais, P.; Saunois, M.; Ganadell, J.G.; Dlugokencky, E.J.; Bergamaschi, P.; Bergmann, D.; Blake, D.R.; Bruhwiler, L.; et al. Three decades of global methane sources and sinks. *Nat. Geosci.* **2013**, *6*, 813–823. [[CrossRef](#)]
3. Anthony, S.E.; Prahl, F.G.; Peterson, T.D. Methane dynamics in the Willamette River, Oregon. *Limnol. Oceanogr.* **2012**, *57*, 1517–1530. [[CrossRef](#)]
4. WMO. *Greenhouse Gas Bulletin*; WMO: Geneva, Switzerland, 2018.
5. Khalil, M.A.K.; Rasmussen, R.A. Sources, sinks, and seasonal cycles of atmospheric methane. *J. Geophys. Res.* **1983**, *88*, 5131–5144. [[CrossRef](#)]
6. Bastviken, D.; Tranvik, L.J.; Downing, J.A.; Crill, P.M.; Enrich-Prast, A. Freshwater methane emissions offset the continental carbon sink. *Science* **2011**, *331*, 50. [[CrossRef](#)]
7. Stanley, E.H.; Casson, N.J.; Christel, S.T.; Crawford, J.T.; Loken, L.C.; Oliver, S.K. The ecology of methane in streams and rivers: Patterns, controls, and global significance. *Ecol. Monogr.* **2016**, *86*, 146–171. [[CrossRef](#)]
8. Wu, S.; Li, S.Q.; Zou, Z.H.; Hu, T.; Hu, Z.Q.; Liu, S.W.; Zou, J.W. High methane emissions largely attributed to ebullitive fluxes from a subtropical river draining a rice paddy watershed in China. *Environ. Sci. Technol.* **2019**, *53*, 3499–3507. [[CrossRef](#)]
9. Tan, Y.J. *The Greenhouse Gases Emission and Production Mechanism from River Sediment in Shanghai*; East China Normal University: Shanghai, China, 2017.
10. Rajkumar, A.N.; Barnes, J.; Ramesh, R.; Purvaja, R.; Upstill-Goddard, R.C. Methane and nitrous oxide fluxes in the polluted Adyar River and estuary, SE India. *Mar. Pollut. Bull.* **2008**, *56*, 2043–2051. [[CrossRef](#)]
11. Yang, L.B.; Li, X.Y.; Yan, W.J.; Ma, P.; Wang, J.N. CH<sub>4</sub> concentrations and emissions from three rivers in the Chaohu Lake watershed in Southeast China. *J. Integr. Agric.* **2012**, *11*, 665–673. [[CrossRef](#)]
12. Liu, K.H.; Hu, Z.B.; Wei, J.Q.; Jiang, Z.; Lu, H.; Wang, C. Analysis of methane flux produced by city black odor river in summer—An example of Chaoyang Creek in Nanjing city, China. *Earth Environ.* **2015**, *43*, 415–419.
13. Qu, B.; Aho, K.S.; Li, C.L.; Kang, S.C.; Sillanpää, M.; Yan, F.P.; Aymond, P.A. Greenhouse gases emissions in rivers of the Tibetan Plateau. *Sci. Rep.* **2017**, *7*, 16573. [[CrossRef](#)]
14. Xiong, Q.L.; Pan, K.W.; Zhang, L.; Wang, Y.J.; Li, W.; He, X.J.; Luo, H.Y. Warming and nitrogen deposition are interactive in shaping surface soil microbial communities near the alpine timberline zone on the eastern Qinghai-Tibet Plateau, southwestern China. *Appl. Soil Ecol.* **2016**, *101*, 72–83. [[CrossRef](#)]
15. Gong, D.L.; Hong, X.; Zeng, G.J.; Wang, Y.; Zuo, S.M.; Liu, X.L.; Wu, J.S. Prediction of water quality in rivers in agricultural regions typical of subtropical in China using Multivariate Linear Regression Model. *J. Ecol. Rural Environ.* **2017**, *33*, 509–518.
16. Wang, Y.; Li, Y.; Liu, F.; Li, Y.Y.; Song, L.F.; Li, H.; Meng, C.; Wu, J.S. Linking rice agriculture to nutrient chemical composition, concentration and mass flux in catchment streams in subtropical central China. *Agric. Ecosyst. Environ.* **2014**, *184*, 9–20. [[CrossRef](#)]
17. Wu, H.B.; Lyu, C.W.; Li, Y.E.; Qin, X.B.; Liao, Y.L.; Li, Y. The spatial-temporal distribution of nitrogen and N<sub>2</sub>O emission from soil and sediment in agricultural watershed of Tuoja River. *Acta Sci. Circumstantiae* **2017**, *37*, 1539–1546.
18. Holmes, M.E.; Chanton, J.P.; Bae, H.S.; Ogram, A. Effect of nutrient enrichment on  $\delta^{13}\text{C}_4$  and the methane production pathway in the Florida Everglades. *Biogeosciences* **2013**, *119*, 1267–1280.



19. Lü, F.; Hao, L.P.; Guan, D.X.; Qi, Y.J.; Shao, L.M.; He, P.J. Synergetic stress of acids and ammonium on the shift in the methanogenic pathways during thermophilic anaerobic digestion of organics. *Water Res.* **2013**, *47*, 2297–2306. [CrossRef]
20. Avery, G.B.; Shannon, R.D.; White, J.R.; Martens, C.S.; Alperin, M.J. Controls on methane production in a tidal freshwater estuary and a peatland: Methane production via acetate fermentation and CO<sub>2</sub> reduction. *Biogeochemistry* **2002**, *62*, 19–37. [CrossRef]
21. Hines, M.E.; Duddleston, K.N.; Rooney-Varga, J.; Fields, D.; Chanton, J.P. Uncoupling of acetate degradation from methane formation in Alaskan wetlands: Connections to vegetation distribution. *Glob. Biogeochem. Cycles* **2008**, *22*. [CrossRef]
22. Hao, L.P.; Lü, F.; He, P.J.; Li, L.; Shao, L.M. Predominant contribution of syntrophic acetate oxidation to thermophilic methane formation at high acetate concentrations. *Environ. Sci. Technol.* **2011**, *45*, 508–513. [CrossRef]
23. Wu, K.; Lu, B.; Yuan, Z. The recent developments and the contribution of farmland irrigation to national grain safeness in China. *J. Irrig. Drain.* **2006**, *25*, 7–10.
24. Zhang, W.; Yu, Y.Q.; Huang, Y.; Li, T.T.; Wang, P. Modeling methane emissions from irrigated rice cultivation in China from 1960 to 2050. *Glob. Chang. Biol.* **2011**, *17*, 3511–3523. [CrossRef]
25. FAO. Statistical databases, Food and Agriculture Organization (FAO) of the United Nations. 2014. Available online: <http://faostat.fao.org/> (accessed on 2 March 2020).
26. Zhu, Z.Y.; Zhang, X.B.; Li, M.X. China's pork market in 2018 and its prospects for 2019. *Agric. Outlook* **2019**, *4*, 6–9.
27. Song, L.F. *Characteristic and Influencing Factorings of Nitrogen and Phosphorus Export in Jinjing Town in Changsha County*; Huazhong Agricultural University: Wuhan, China, 2014.
28. Seitzinger, S.P.; Kroeze, C. Global distribution of nitrous oxide production and N inputs in freshwater and coastal marine ecosystems. *Glob. Biogeochem. Cycles* **1998**, *12*, 93–113. [CrossRef]
29. Zou, J.W.; Huang, Y.; Jiang, J.Y.; Zheng, X.H.; Sass, R.L. A 3-year field measurement of methane and nitrous oxide emissions from rice paddies in China: Effects of water regime, crop residue, and fertilizer application. *Glob. Biogeochem. Cycles* **2005**, *19*, 1–9. [CrossRef]
30. Li, J.L.; Li, Y.E.; Wan, Y.F.; Wang, B.; Waqas, M.A.; Cai, W.W.; Guo, C.; Zhou, S.H.; Su, R.S.; Qin, X.B.; et al. Combination of modified nitrogen fertilizers and water saving irrigation can reduce greenhouse gas emissions and increase rice yield. *Geoderma* **2018**, *315*, 1–10. [CrossRef]
31. Yuan, M.D. *Methanogenesis and Nitrogen Removal in the Biological Stabilization Ponds for Large Scale Swine Wastewater Treatment*; Zhejiang University: Hangzhou, China, 2016.
32. Xu, W.Q. *Study and Estimation on the Biochemical Methane Potential of Livestock Manure in Anaerobic Digestion*; Chinese Academy of Agricultural Sciences Dissertation: Beijing, China, 2017.
33. Tian, D.; Jiang, L.; Ma, S.H.; Fang, W.J.; Schmid, B.; Xu, L.C.; Zhu, J.X.; Li, P.; Losapio, G.; Jing, X.; et al. Effects of nitrogen deposition on soil microbial communities in temperate and subtropical forests in China. *Sci. Total Environ.* **2017**, *607–608*, 1367–1375. [CrossRef]
34. Borges, A.V.; Darchambeau, F.; Lambert, T.; Bouillon, S.; Morana, C.; Brouyère, S.; Hakoun, V.; Jurado, A.; Tseng, H.C.; Descy, J.P.; et al. Effects of agricultural land use on fluvial carbon dioxide methane and nitrogen oxide concentrations in a large European river, the Meuse (Belgium). *Sci. Total Environ.* **2018**, *610–611*, 342–355. [CrossRef]
35. Wu, H.B. *Greenhouse Gas Emission and Transport of Carbon and Nitrogen in Typical River Ecosystem*; Anhui Normal University: Wuhu, China, 2017.
36. Qin, X.B.; Li, Y.; Goldberg, S.; Wan, Y.F.; Fan, M.R.; Liao, Y.L.; Wang, B.; Gao, Q.Z.; Li, Y.E. Assessment of indirect N<sub>2</sub>O emission factors from agricultural river networks based on long-term study at high temporal resolution. *Environ. Sci. Technol.* **2019**, *53*, 10781–10791. [CrossRef]
37. Qin, X.B.; Li, Y.E.; Wan, Y.F.; Fan, M.R.; Liao, Y.L.; Li, Y.; Wang, B.; Gao, Q.Z. Diffusive flux of CH<sub>4</sub> and N<sub>2</sub>O from agricultural river networks: Regression tree and importance analysis. *Sci. Total Environ.* **2020**, *717*, 137244. [CrossRef]
38. Zhao, Q.; Lyu, C.W.; Qin, X.B.; Wu, H.B.; Wan, Y.F.; Liao, Y.L.; Lu, Y.H.; Wang, B.; Li, Y. Key pathway of methane production and characteristics of stable carbon isotope of the Tuoja River waterbody. *Chin. J. Appl. Ecol.* **2018**, *29*, 1450–1460.

39. Liss, P.S.; Merlivat, L. Air-sea gas exchange rates: Introduction and synthesis. *Role Air Sea Exch. Geochem. Cycl.* **1986**, *185*, 113–127.
40. Zhang, Y.; Li, Y.; Qin, X.B.; Kong, F.L.; Chi, M.; Li, Y.E. Dissolved methane concentration and emission flux in agricultural watershed of subtropics. *Sci. Agric. Sin.* **2016**, *49*, 3968–3980.
41. Raymond, P.A.; Cole, J.J. Gas exchange in rivers and estuaries: Choosing a gas transfer velocity. *Estuary Coast* **2001**, *24*, 312–317. [[CrossRef](#)]
42. Wanninkhof, R. Relationship between wind speed and gas exchange over the ocean. *J. Geophys. Res. Ocean.* **1992**, *97*, 7373–7382. [[CrossRef](#)]
43. Huttunen, J.T.; Väisänen, T.S.; Hellsten, S.K.; Martikainen, P.J. Methane fluxes at the sediment-water interface in some boreal lakes and reservoirs. *Boreal Environ. Res.* **2006**, *11*, 27–34.
44. Koné, Y.J.M.; Abril, G.; Delille, B.; Borges, A.V. Seasonal variability of methane in the rivers and lagoons of Ivory Coast (West Africa). *Biogeochemistry* **2010**, *100*, 21–37. [[CrossRef](#)]
45. Teodoru, C.R.; Nyoni, F.C.; Borges, A.V.; Darchambeau, F.; Nyambe, I.; Bouillon, S. Spatial variability and temporal dynamics of greenhouse gas (CO<sub>2</sub>, CH<sub>4</sub>, N<sub>2</sub>O) concentrations and fluxes along the Zambezi River mainstem and major tributaries. *Biogeosci. Discuss.* **2014**, *11*, 16391–16445. [[CrossRef](#)]
46. Zhang, G.L.; Zhang, J.; Liu, S.M.; Ren, J.L.; Xu, J.; Zhang, F. Methane in the Changjiang (Yangtze River) Estuary and its adjacent marine area: Riverine input, sediment release and atmospheric fluxes. *Biogeochemistry* **2008**, *91*, 71–84. [[CrossRef](#)]
47. Schade, J.D.; Bailio, J.; McDowell, H. Greenhouse gas flux from headwater streams in New Hampshire, USA: Pattern and drivers. *Limnol. Oceanogr.* **2016**, *61*, S165–S174. [[CrossRef](#)]
48. Gao, X.X. *Study on Methane Flux Emitted from Manure Pond on Medium Scale Pig Farm*; Chinese Academy of Agricultural Science: Beijing, China, 2007.
49. Siczko, A.K.; Demeter, K.; Singer, G.A.; Tritthart, M.; Preiner, S.; Mayr, M.; Meisterl, K.; Peduzzi, P. Aquatic methane dynamics in a human-impacted river-floodplain of the Danube. *Limnol. Oceanogr.* **2016**, *61*, S175–S181. [[CrossRef](#)]
50. Chen, H.; Zhou, S.; Wu, N.; Wang, Y.F.; Luo, P.; Shi, F.S. Advance in studies on production, oxidation and emission flux of methane from wetlands. *Chin. J. Appl. Environ. Biol.* **2006**, *12*, 726–733.
51. Yang, S.S.; Chen, I.C.; Liu, C.P.; Liu, L.Y.; Chang, C.H. Carbon dioxide and methane emissions from Tanswei River in Northern. *Atmos. Pollut. Res.* **2015**, *6*, 52–61. [[CrossRef](#)]
52. Schrier-Uijl, A.P.; Veraart, A.J.; Leffelaar, P.A.; Berendse, F.; Veenendaal, E.M. Release of CO<sub>2</sub> and CH<sub>4</sub> from lakes and drainage ditches in temperate wetlands. *Biogeochemistry* **2011**, *102*, 265–279. [[CrossRef](#)]
53. Mer, J.L.; Roger, P. Production, oxidation, emission and consumption of methane by soils: A review. *Eur. J. Soil Biol.* **2001**, *37*, 25–50. [[CrossRef](#)]
54. Bodelier, P.L.E.; Laanbroek, H.J. Nitrogen as a regulatory factor of methane oxidation in soils and sediments. *FEMS Microbiol. Ecol.* **2004**, *47*, 265–277. [[CrossRef](#)]
55. Galbally, I.E.; Kirstine, W.V.; Meyer, C.P.; Wang, Y.P. Soil-atmosphere trace gas exchange in semiarid and arid zones. *J. Environ. Qual.* **2008**, *37*, 599–607. [[CrossRef](#)]
56. Kuivila, K.M.; Murray, J.W.; Devol, A.H. Methane production, sulfate reduction and competition for substrates in the sediments of Lake Washington. *Geochim. Cosmochim. Acta* **1989**, *53*, 409–416. [[CrossRef](#)]
57. Heilman, M.A.; Carlton, R.G. Ebullitive release of lacunar gases from floral spikes of *Potamogeton angustifolius* and *Potamogeton amplifolius*: Effects on plant aeration and sediment CH<sub>4</sub> flux. *Aquat. Bot.* **2001**, *71*, 19–33. [[CrossRef](#)]
58. Crowe, S.A.; Katsev, S.; Leslie, K.; Sturm, A.; Magen, C.; Nomosatryo, S.; Pack, M.A.; Kessler, J.D.; Reeburgh, W.S.; Roberts, J.A.; et al. The methane cycle in ferruginous Lake Matano. *Geobiology* **2011**, *9*, 61–78. [[CrossRef](#)]
59. Oswald, K.; Milucka, J.; Brand, A.; Littmann, S.; Wehrli, B.; Kuypers, M.M.M.; Schubert, C.J. Light-dependent aerobic methane oxidation reduces methane emission from seasonally stratified lakes. *PLoS ONE* **2015**, *10*, e0132574. [[CrossRef](#)]
60. Reeburgh, W.S. Oceanic methane biogeochemistry. *Chem. Rev.* **2007**, *107*, 486–513. [[CrossRef](#)] [[PubMed](#)]
61. Ding, W.X.; Cai, Z.C.; Tsuruta, H. Plant species effects on methane emissions from freshwater marshes. *Atmos. Environ.* **2005**, *39*, 3199–3207. [[CrossRef](#)]
62. Zhu, Z.L.; Xing, G.X. *Nitrogen Cycling*; Tsinghua University Press: Beijing, China, 2002.

63. Bagoon, D.; Jones, R.D. Potential rates of methanogenesis in sawgrass marshes with peat and marl soils in the Everglades. *Soil Biol. Biochem.* **1992**, *24*, 21–27. [[CrossRef](#)]
64. Wright, A.L.; Reddy, K.R. Phosphorus loading effects on extracellular enzyme activity in Everglades wetland soils. *Soil Sci. Soc. Am. J.* **2001**, *65*, 588–595. [[CrossRef](#)]
65. Kelly, C.A.; Chynoweth, D.P. The Contributions of temperature and of the input of organic matter in controlling rates of sediment methanogenesis. *Limnol. Oceanogr.* **1981**, *26*, 891–897. [[CrossRef](#)]
66. Chin, K.J.; Lukow, T.; Conrad, R. Effect of temperature on structure and function of the methanogenic archaeal community in an anoxic rice field soil. *Appl. Environ. Microbiol.* **1999**, *65*, 2341–2349. [[CrossRef](#)]
67. Venkiteswaran, J.J.; Rosamond, M.S.; Schiff, S.L. Nonlinear response of riverine N<sub>2</sub>O fluxes to oxygen and temperature. *Environ. Sci. Technol.* **2014**, *48*, 1566–1573. [[CrossRef](#)]
68. Zeng, F.W.; Masiello, C.A.; Hockaday, W.C. Controls on the origin and cycling of riverine dissolved inorganic carbon in the Brazos River, Texas. *Biogeochemistry* **2011**, *104*, 275–291. [[CrossRef](#)]
69. Dyson, K.E.; Billett, M.F.; Dinsmore, K.J.; Harvey, F.; Thomson, A.M.; Piirainen, S.; Kortelainen, P. Release of aquatic carbon from two peatland catchments in E. Finland during the spring snowmelt period. *Biogeochemistry* **2011**, *103*, 125–142. [[CrossRef](#)]
70. Conrad, R. Contribution of hydrogen to methane production and control of hydrogen concentrations in methanogenic soils and sediments. *FEMS Microbiol. Ecol.* **1999**, *28*, 193–202. [[CrossRef](#)]
71. Whiticar, M.J. Carbon and hydrogen isotope systematics of bacterial formation and oxidation of methane. *Chem. Geol.* **1999**, *161*, 291–314. [[CrossRef](#)]



© 2020 by the authors. Licensee MDPI, Basel, Switzerland. This article is an open access article distributed under the terms and conditions of the Creative Commons Attribution (CC BY) license (<http://creativecommons.org/licenses/by/4.0/>).